ROYAL SOCIETY
OF CHEMISTRY

PAPER

Check for updates

Reducing gas-loss in rigid polyisocyanurate foams using metal–organic frameworks

Michael S. Harris, [ID] Jonathan A. Foster [ID] * and Anthony J. Ryan*

Polyisocyanurate (PIR) foams are widely used to insulate buildings, but their performance reduces over time leading to wasted energy and higher heating costs. High molecular weight gases used to blow the foams gradually diffuse out and are replaced by air leading to an increase in thermal conductivity. A wide variety of additives have been tested to improve the barrier properties of polymers including metal–organic frameworks (MOFs) which have proved promising candidates thanks to their tunable surface chemistry. In this work, a new and robust method for determining gas loss from rigid PIR foams has been developed, and utilised to determine the effect of different MOF additives on gas loss. An accelerated ageing method was developed, in which the mass of a fixed volume of foam was kept in an oven at 70 °C and weighed at 24 hour time intervals. This was found to provide reproducible measurements of gas loss over a period of 28 days with a variation of 1.1% by mass for typical samples. Five different MOFs were added to polyisocyanurates, and their effects on cell size, closed cell content, and gas loss over time were measured. Cu(ABDC)(DMF) was found to enhance the gas retention of PIR foams with minimal change to cell size or closed cell content. A modulated (flower-like) NH_2-MIL-53 MOF increased the closed cell fraction whilst reducing cell size, with no effect on gas loss, whilst an unmodulated (cube like) NH_2-MIL-53 MOF increased the gas loss without affecting cell size or closed cell percentage. Two further MOFs, Cu(BTetC)(DMF) and Cu(BDC)(DMF), were found to have no effect. This work therefore identifies Cu(ABDC)(DMF) as a promising additive for reducing gas-loss and maintaining the long-term performance in PIR foams, with its effectiveness demonstrated via an accelerated ageing technique developed for this study.

1. Introduction

The building sector accounts for 25–40% of total global energy consumption,[1–5] and 30–50% of greenhouse gas emissions.[5–8] The United Nations Environmental Programme (UNEP) has estimated that energy consumption in buildings can be reduced by 30–80%[9] by utilising technologies such as more efficient boilers,[10] heat pumps[11] and solar panels.[12] However, the most effective route to reducing CO_2 emissions from buildings is to improve insulation, which allows the building to remain at a habitable temperature without minimising heat exchange to the outdoors.[13–15]

A variety of materials are used for insulation, and their choice largely depends on factors such as geographical location,[16] price,[16,17] and available space.[18] The most widely used polymeric material worldwide for insulation is polyisocyanurates (PIR) due to their low thermal conductivity, high strength compared to weight, adhesive properties, and durability for installation.[19–21]

School of Mathematical and Physical Sciences and The Grantham Centre for Sustainable Futures, University of Sheffield, S10 1TN Sheffield, England. E-mail: jona.foster@sheffield.ac.uk, tony.ryan@sheffield.ac.uk

Polymeric foam insulating materials utilise a polymer to create a solid matrix of bubbles (known as cells), formed by an expansion or production of a gas (blowing agent).

Radiation, conduction, and convection[22–24] are the primary routes through which heat can be transferred in insulating materials.[22–25] More than 50% of heat transfer in a PIR foam comes directly from convection of the blowing agent within the foam cells.[26,27] Blowing agents are therefore chosen with low K (thermal conductivity) values to minimise heat transfer. However, blowing agents have been shown to diffuse out of the foam over time and are replaced by air which has a higher K value. This leads to a reduction in the performance of the insulation.[27–30] Research into the diffusion of blowing agent from PIR foams has been studied with CFCs being monitored from legacy PIR foams[31] or the change in thermal conductivity of PIR foam over 400 days.[32] However, research into prevention of this diffusion between cells is limited, with no standardised testing available, or materials to reduce the gas loss over time. This work investigates the use of additives within PIR foams to either prevent, or slow down, the rate of blowing agent diffusion.[32,33] Metal–organic frameworks were chosen as the additives to create new PIR composites.

Metal–organic frameworks (MOFs) are co-ordination networks consisting of organic ligands coordinated to metal ions or clusters that contain potential voids.[33–35] MOFs can be synthesised from a variety of metal centres and linkers. For example, linkers can be carboxylate based, N-donor based, and phosphine based, while examples of metal centres are copper, aluminium, zinc, hafnium and zirconium, with different combinations of linkers and metals resulting in different MOFs.[34,36–43] This modular approach to the design and synthesis of MOFs allows for extremely tuneable materials.[44,45] Applications of MOFs in polymers focus on gas separation[46–48] and gas storage.[49–51] Copper and aluminium terephthalic acid based MOFs have been regularly used in polymers for gas separation, typically with polyimides, to separate CO_2/CH_4 resulting in increased selectivity or permeance of membranes.[52,53] However, little work has been done on incorporating these MOFs into PIR. Typical blowing agents in PIR are pentanes,[22] therefore, copper and aluminium terephthalic acid based MOFs could offer some barrier properties when included in PIR.

This work aims to demonstrate a method for the monitoring of gas loss from rigid PIR foams within a short timeframe, and determine if tailored materials, MOFs, can be introduced to PIR foams to reduce their gas loss over time. Specifically, this work will utilise accelerated ageing of PIR foams at 70 °C and use common PIR additives molybdenum disulphide and graphite as solid particulates for validation of the method. Then MOFs Cu(BDC)(DMF), Cu(ABDC)(DMF), Cu(BTetC)(DMF) and NH2-MIL-53 (modulated and unmodulated) will be used to determine if gas loss from PIR foams can be reduced.

Results and discussion

Determining gas loss from PIR foam

Accelerated ageing at high temperatures has been used in industry to monitor changes in performance (such as thermal conductivity) over time;[54] however, to our knowledge there are no reported methods in the literature for directly measuring gas loss. This work proposes a method of accelerated ageing that can be used to determine the mass loss and therefore infer gas loss from PIR foams by monitoring the mass change of a PIR foam kept in a 70 °C environment (Fig. 1).

Several different methods were initially tested, including gas cell analysis with PIR membranes, headspace analysis of cut PIR foam cubes, and vacuum ageing of PIR foam. The following method was chosen based on preliminary work and found to provide the most accurate and reliable measurements, so was used throughout the study. PIR foam was synthesised on a 100 g scale in a 1 L disposable paper cup. The head (any foam that had risen beyond the rim of the cup) was then removed. Foams were kept inside the cup for ageing and analysis, which provides a regular, singular exposed surface for gasses to escape (Fig. 1). To allow for further regularity across the samples, each foam was synthesised, allowed to settle (from any temperature or reactive effects) for 24 hours, then cut using a foam saw and allowed to settle for a further 24 hours. These cut foam cups were then placed in a closed oven and weighed daily over the course of 28 days at a minimum. Three replicates were performed and used to calculate the mean average.

To understand the effect of accelerated ageing, a reference sample was made and monitored at room temperature alongside an accelerated sample at 70 °C for 28 days. Fig. 2a shows the average % mass loss over time for these samples, where the room temperature environment foam shows a slight increase in mass over 28 days, whilst the foam placed into an oven demonstrates a logarithmic loss of mass. The slight increase in mass is attributed to moisture adsorption by the foam when kept under ambient conditions which exceeds any loss of blowing agent consistent with slow release at this temperature. The higher temperature used in the accelerated ageing method therefore offered robust analysis of the mass loss, which in turn provided insights into gas loss from the foam over time, making it a successful development in foam analysis. This technique was then utilised for the analysis of composite foams.

Validation of accelerated ageing method on composite foams

To validate the method developed, two materials were purchased as model additives to introduce into the foams: MoS_2 and graphite. Both materials have been used in gas barrier
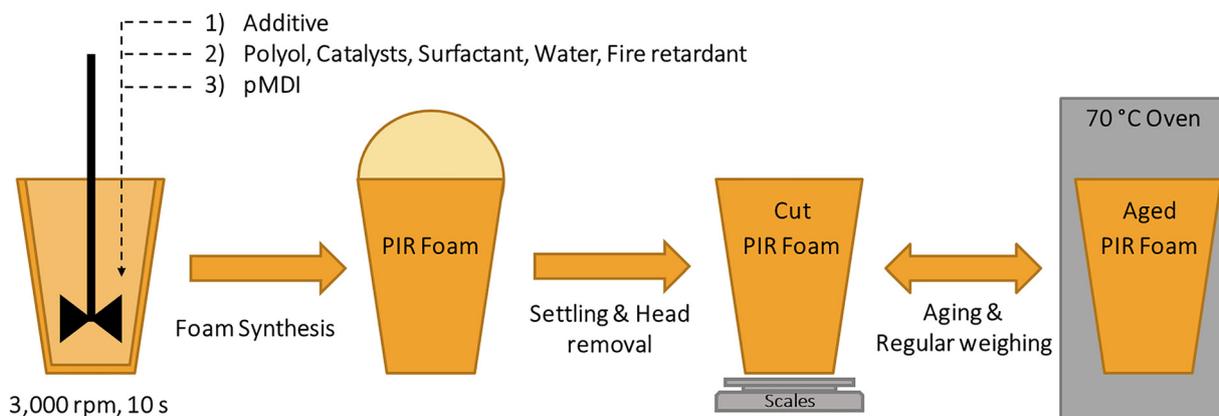

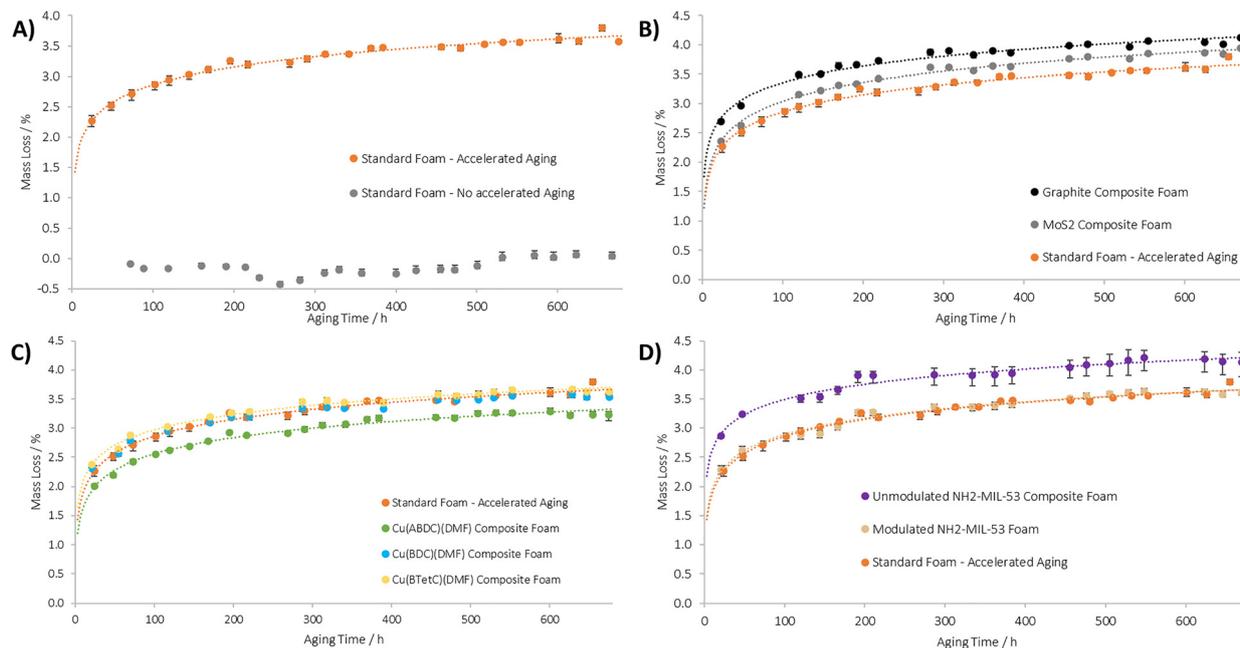Fig. 1 Scheme showing methods used for the synthesis and accelerated ageing of PIR foams.

Fig. 2 Mass loss from rigid PIR foams over time. (A) Mass loss under ambient or accelerated conditions. (B) Compared to MoS_2 and graphite composites. (C) Compared to copper MOF composites. (D) Compared to aluminium MOF composites.

applications where the inclusion of the additives reduced permeation through polyurethanes.[55–57] They have also been used in foam applications where these additives can increase other properties such as hydrophobicity,[58] mechanical strength,[58] or electrical conductivity[59] of polyurethane foams. This makes them the ideal initial testing materials for validation of the accelerated ageing technique.

For determining the optimal loading of additives to the PIR foam, helium pycnometry analysis was utilised to establish the fraction of closed cells of the foams produced. Additives are known to act as cell openers in PIR foams.[60] A higher open cell fraction results in an easier pathway for the blowing agent to leave, reducing the lifetime efficiency of the foam. The standard PIR foam produced without additives demonstrated a high closed cell content of $85 \pm 1\%$. The addition of high loadings (>0.1 wt %) of MoS2 or graphene additives produced foams with much lower closed cell content (72% closed at 5 wt% and 82% closed at 1 wt% respectively for MoS_2 composites (Fig. S2, SI)). The drop in closed cell fraction was attributed to cell opening via solid particulate dewetting.[61] Therefore, 0.1% by weight loadings were targeted, a graphite and a MoS_2 foam produced a highly closed cell foam (graphite at $84 \pm 3\%$, MoS_2 at $86 \pm 1\%$).

Fig. 2b shows the mass loss of 3 sets of foams: a pure foam, a composite foam containing MoS_2 at 0.1% loading, and a composite foam containing graphite at a 0.1% loading. In all cases the logarithmic decay of the mass loss is seen, with both the MoS_2 and graphite foams having a greater mass loss ($3.94 \pm 0.00\%$ and $4.12 \pm 0.02\%$ respectively at 28 days) over time than the pure foam ($3.58 \pm 0.04\%$ at 28 days).

Other additives have been found to have significant effects on The increased mass loss over time for the composite foams may be attributed to the slight increase in cell size (Fig. 4), though the values were within error in both composite foams when compared to the standard foams. Alternatively, the introduction of the additive could have led to the creation of voids in the polymer matrix, creating more channels for the blowing agent to travel through the cell walls more efficiently.[62] Overall, it can be concluded that this analysis technique is suitable for analysing the barrier properties of the composites, and low percentages of additive introduced to PIR can have effects on gas retention without disruption of either closed cell percentage or cell size. This method could be utilised for a variety of additives, or other highly closed cell foams.

Effect of MOFs on gas loss

This section aims to determine if tailored materials, MOFs, can be introduced to PIR foams to reduce their gas loss over time. Three copper MOF systems were utilised for 0.1% weight PIR composites: Cu(BDC)(DMF) (where BDC is 1,4-benzenedicarboxylate linker and DMF is the co-ordinated solvent dimethyl formamide), Cu(ABDC)(DMF) (where ABDC is 2-amino-1,4-benzenedicarboxylate) and Cu(BTetC)(DMF) (where BTetC is a 1,2,4,5-benzene tetracarboxylate). Two aluminium MOFs were also utilised for 0.1% weight composites. These consisted of NH_2-MIL-53 (synthesis adapted from the work by Jinhuai Liu et al.[63]), and a modulated version of NH_2-MIL-53 produced with a flower-like structure (Fig. 3) resulting in a distinct morphology.[63] These MOFs were chosen for their previous use in polymers, facile synthesis and their relation to one another allowing for investigation into different possible effects, such as surface chemistry, morphology and density. All MOFs were synthesised according to previously reported methods (Fig. 3). All MOFs were found to be pure via powder X-ray diffraction and elemental analysis.
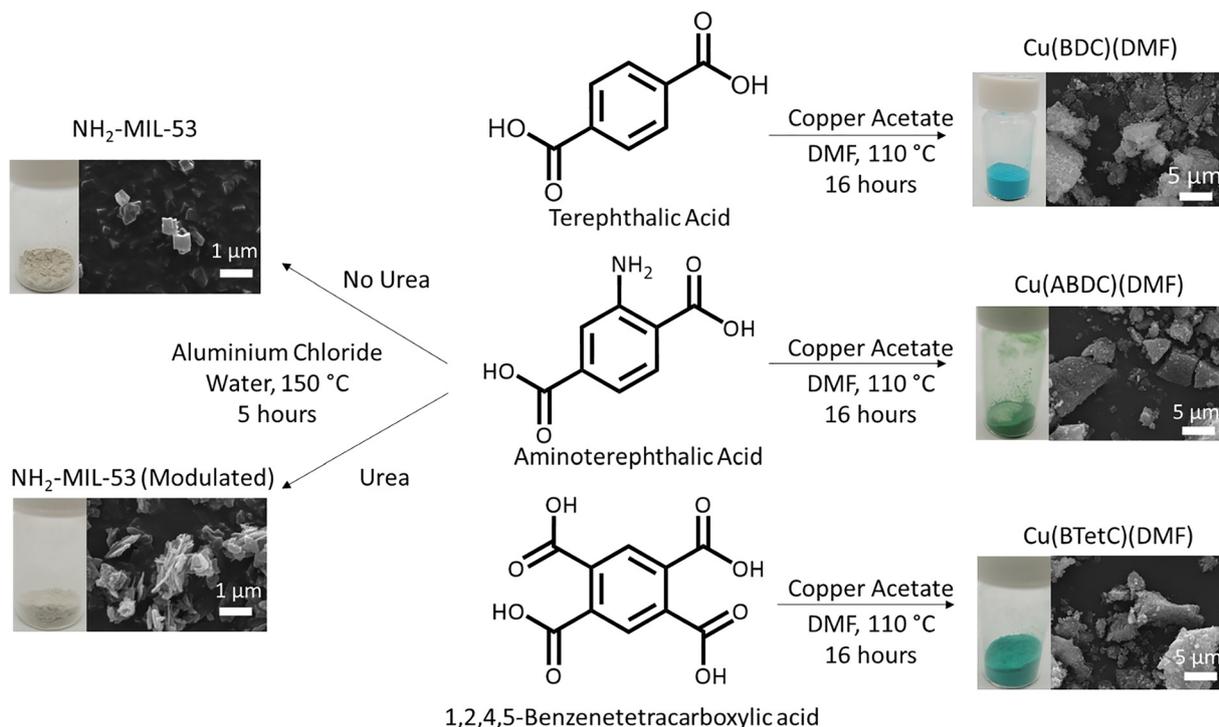
Fig. 3 Reaction schemes for the synthesis of Cu(BDC)(DMF), Cu(ADC)(DMF), Cu(BTetC)(DMF), NH$_2$-MIL-53 and modulated NH$_2$-MIL-53.

Fig. 2c shows the mass loss of different composite foams containing Cu MOF additives, and Fig. 2d containing the Al MOF additives. Each curve shows a logarithmic decay, like that observed for the standard PIR foam, those of PIR MoS$_2$/graphite composites. Mass loss from the MOF composites after 28 days showed improved performance (decreased mass loss) by the addition of Cu(ABDC)(DMF). Addition of other MOFs resulted in little change in the gas loss compared to the standard foam. Addition of unmodulated NH$_2$-MIL-53 resulted in decreased performance (increased mass loss) compared to the standard foam.

To understand the effect that the different MOFs had on the structure of the foam, the average cell size was measured *via* SEM and the closed cell content measured by pycnometry (Table 1). Closed cell content was unchanged within experimental error for all samples (around 85%), except for samples containing modulated NH$_2$-MIL-53 which showed a substantial increase (to 94 ± 4%). The average cell size was also within experimental error for all samples except the modulated NH$_2$-MIL-53 composite, which demonstrated significant reductions in cell size (154 ± 18 μm) compared to the base foam (222 ± 27 μm) seen in Fig. 4.

Direct comparison between the MOF additives is challenging due to differences in functionality, but also morphology and particle size. The key outliers to explain are the improved performance on addition of Cu(ABDC)(DMF) and the reduced performance of unmodulated NH$_2$-MIL-53 but not modulated NH$_2$. The Cu based MOFs have a dense morphology due to the co-ordinated DMF molecules of one-layer sitting inside the pores of the layers above and below. Our initial hypothesis was therefore that incorporation of these MOFs into the walls of
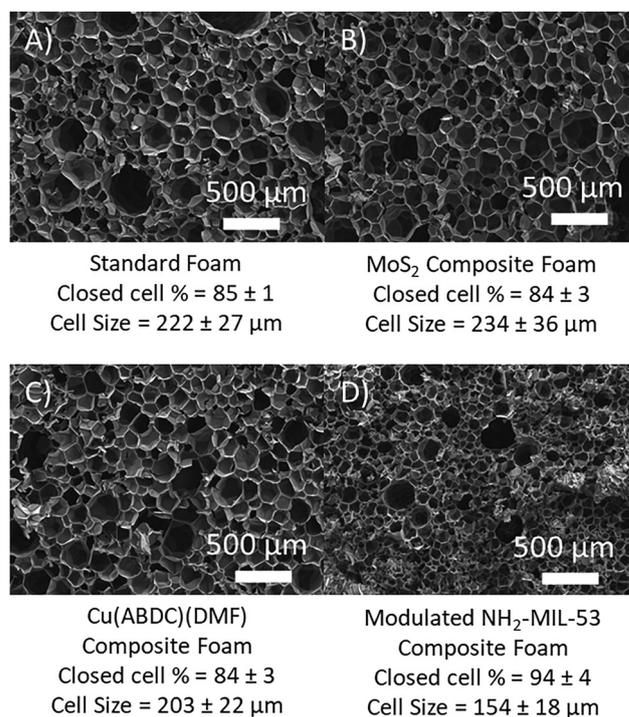

Fig. 4 SEM images of (A) standard PIR foam, (B) MoS$_2$ composite foam, (C) Cu(ABDC)(DMF) composite foam, (D) modulated NH$_2$-MIL-53 composite foam.

the PIR foam would improve barrier properties by creating a tortuous path around which escaping gasses would have to flow. We suggest that the enhanced performance of Cu(ABDC)(DMF),

Table 1 Closed cell, cell size and mass lost at 28 days of PIR and composite PIR foams. Increased values are denoted in bold with ^, decreased values denoted in italics with *

Foam additive	Closed cells/%	Cell size/μm	Mass loss at 28 days per g
None	85 ± 1	222 ± 27	3.58 ± 0.04
MoS₂	84 ± 3	234 ± 36	**3.94 ± 0.00^**
Graphite	86 ± 1	230 ± 29	**4.12 ± 0.02^**
Cu(BDC)(DMF)	88 ± 7	190 ± 23	3.54 ± 0.05
Cu(BtetC)(DMF)	85 ± 1	195 ± 17	3.62 ± 0.03
Cu(ABDC)(DMF)	84 ± 3	203 ± 22	*3.22 ± 0.09**
NH₂-MIL-53 unmodulated	84 ± 5	*179 ± 17**	**4.14 ± 0.22^**
NH₂-MIL-53 modulated	**94 ± 4^**	*154 ± 18**	3.61 ± 0.05

but not the other Cu based MOFs, is likely due to the amino-functional group reacting with the isocyanates of the setting PIR foam enabling enhanced incorporation within the matrix.

Amino groups are also present in the two NH$_2$-MIL-53 systems, so another explanation is required here. In contrast to the dense Cu MOFs, the MIL-53 system has an open "wine-rack" like structure,[63] with channels running through it which have been utilised for CO$_2$[64–66] capture, in separation applications of CO$_2$ and CH$_4$[67,68] and adsorption of hydrocarbons.[69] It is therefore likely that blowing agents (iso- and cyclo- pentane) could be transported through these channels more easily than the polymer matrix, enhancing gas loss. This would explain the increase in the rate of gas loss seen for un-modulated NH$_2$-MIL-53. Modulated NH$_2$-MIL-53 might be expected to show similar behaviour, however a confounding factor in this case is that addition of the MOFs results in changes in closed cell fraction and cell size. Cell size decreases most significantly for the modulated NH$_2$-MIL-53, which is expected to reduce gas loss as blowing agents will have to travel through a greater number of cell walls to escape the foam. Closed cell-content also increased for the modulated NH$_2$-MIL-53, which would further enhance this effect reducing escape. We therefore suggest this these effects counteract any increase in gas-loss caused by the presence of the porous MOFs, resulting in little net change in the rate of gas-loss compared to the unmodified foam.

Conclusions

In conclusion, gas loss from PIR foams is a major route to loss in insulation performance over time, resulting in less effective retention of heat. Here, we developed a reproducible method to measure gas loss from PIR foams during accelerated ageing, *via* regular weighing of the foam when placed in an oven at 70 °C. This method allowed for comparison of different inorganic and MOF additives as barrier materials at a 0.1 wt% loading.

A variety of MOFs were synthesised and successfully incorporated at a 0.1 wt% loading into rigid PIR foams. The addition of MOFs drastically altered the loss of blowing agent from the foams depending on the specific MOF utilised. Importantly, addition of Cu(ABDC)(DMF) resulted in reduced gas-loss, showing 3.22 ± 0.09% mass loss after 28 days compared to 3.58 ± 0.04% of the base foam, and 4.14 ± 0.22% of the worst

performing samples. Comparison between the structure of the MOFs and performance of the composite foams indicate functional groups and particle shape are key to determining performance.

These results indicate that MOFs are promising additive for reducing blowing agent loss from PIR foams. We anticipate that the diversity and tunability of MOFs, combined with the simple and highly reproducible methods developed during this study will enable the development of new additives which will improve the lifetime performance of insulation.

Experimental

Materials and characterisation

All materials for foam synthesis were provided by Kingspan (Leominster, UK). Dimethyl formamide (DMF) (> 99%) was purchased from Fisher Scientific (Loughborough, UK). Copper acetate monohydrate (98+ %), aluminium chloride hexahydrate (99%) and 2-aminoterephthalic acid (99%) were purchased from Alfa Aesar (Heysham, UK). Terephthalic acid (99+ %) was purchased from Acros organics (Geel, Belgium). 1,2,4,5-Benzenetetra-carboxylic acid (96%) was purchased form Sigma Aldrich (Dorset, UK). All characterisation methods can be found in the SI.

Foam synthesis and accelerated ageing

Rigid PIR foam is synthesised according to Kingspan's formulation, with all chemicals provided by Kingspan. A "part A" is initially mixed using a polyol, cyclopentane, isopentane, a trimerization catalyst, a surfactant, a flame retardant, and water in a 1 L paper Kingspan cup. Once blended using an overhead stirrer (3000 rpm, 10 seconds), pMDI, "part B", is added on top of the part A mixture and then blended again (3000 rpm, 10 seconds). The total mass of the mixture is 100 g when all components are mixed. For composite foams, the total mass is reduced to accommodate the percentage loading of the additive chosen (*e.g.* a 0.1% loading will use a total of 99.9 g of foam formulation and 0.1 g of additive). The additive is incorporated into the part A mixture as a dry powder prior to mixing.

For accelerated ageing measurements, after the foam had stopped rising, it was left to cool for 24 hours. The head of the foam (all foam above the lip of the cup) was then removed by cutting with an insulation saw. The decapitated foam is again left to rest for a further 24 hours before a baseline weight was obtained. The foam was then placed into an oven at 70 °C and periodically weighed on a balance with a tolerance of ±0.001 g over 28 days.

Synthesis of copper MOFs

Copper acetate monohydrate and linker were separately dissolved in DMF (95 mL) (see SI, Table S1). After dissolution, the solutions were combined and stirred at 110 °C under nitrogen for 16 hours. The reaction mixture was centrifuged (12 000 rpm, 10 min), the supernatant removed, and the solids washed *via* centrifugation (12 000 rpm, 10 min) in DMF (3 × 30 mL), then diethyl ether (3 × 30 mL). The sample was dried under desiccation, producing MOF.

Cu(BCD)(DMF), light blue powder, yield 49.6% (based on Cu). Elemental analysis: calculated mass for $CuC_{12}H_{12}NO_5$%: C 43.89; H 3.75; N 4.654. Found mass %: C 43.52; H 3.76; N 4.58. Phase purity confirmed by PXRD (flat plate) comparison (CCDC entry 687690).[70]

Cu(BTetC)(DMF), teal powder, yield 58.9% (based on Cu). Elemental analysis: calculated mass for $CuC_8H_9NO_5$%: C 36.88; H 3.17; N 5.20; found mass %: C 36.48; H 3.49; N 5.55. Phase purity confirmed by PXRD (flat plate) comparison (CCDC entry 640755).[71]

Cu(ABDC)(DMF), green powder, yield: 84.4% (based on Cu). Elemental analysis: calculated mass for $CuC_{11}H_{13}N_2O_5$%: C 41.85; H 3.89; N 8.63; found mass %: C 41.43; H 3.97; N 8.58. Phase purity confirmed by PXRD (flat plate) comparison (CCDC entry 687690).[70]

Synthesis of aluminium MOFs

Aluminium chloride hexahydrate (0.966 g, 4.00 mmol) and aminoterephthalic acid (0.543 g, 3.00 mmol) are mixed in water (30 mL) for 30 minutes. For modulated NH_2-MIL-53, urea (0.390 g, 6.50 mmol) was added to the reaction mixture and stirred for an additional 30 minutes. The reaction mixture was then transferred to a Teflon lined autoclave and heated to 150 °C for 5 hours with a heating and cooling rate of 10 °C min^{-1}. The yellow solution was then centrifuged (12 000 rpm, 10 min) to yield a yellow solid. For activation, the product was suspended in DMF (50 mL) with stirring at 110 °C for 16 hours then centrifuged (12 000 rpm 10 min). The off-white product was then suspended in methanol (50 mL) and stirred under reflux for 16 hours. Finally, the product was centrifuged (12 000 rpm 10 min) and dried under vacuum at 40 °C for 16 hours, resulting in an off-white powder of NH_2-MIL-53. Unmodulated yield: 88.3% (based on Al), modulated yield: 81.8% (based on Al). Elemental analysis: calculated mass for unmodulated $AlC_8H_8NO_6$%: C 39.84; H 3.32; N 5.81; Found mass %: C 43.50; H 3.89; N 6.09. Calculated mass for modulated $AlC_8H_8NO_6$%: C 39.84; H 3.32; N 5.81; found mass %: C 30.74; H 3.69; N 5.43. Phase purity confirmed by PXRD (flat plate) comparison (CCDC entry 220475)[72] and comparison to paper by Jinhuai Liu et al.[63]

Analysis of MOFs

After synthesis of all MOFs PXRD analysis was completed to determine any phase impurities that may exist in the structure (see SI, Fig. S4.1–3), and a digested (where the MOF was broken down via acid/base into free linker and metal ions in solution) sample was created for NMR to determine if any impurities were in the pores of the MOF (see SI, Fig. S3.1–3). Finally, FT-IR measurements were also performed to determine any impurities (see SI, Fig. S5.1–3). DLS measurements in solvent after dispersion with sonication (37 kHz for 60 seconds) were also performed to provide additional sizing measurements (see SI, Fig. S6.1–3)

Author contributions

Conceptualisation, M. S. H., J. A. F., and A. J. R.; methodology M. S. H.; formal analysis, M. S. H.; investigation, M. S. H.; data

curation, M. S. H.; writing – original draft preparation, M. S. H.; writing – review and editing, J. A. F. and A. J. R.; visualisation, M. S. H.; supervision, J. A. F. and A. J. R.; funding acquisition, J. A. F and A. J. R. All authors have read and agreed to the published version of the manuscript.

Conflicts of interest

There are no conflicts to declare.

Data availability

The data supporting this article have been included as part of the supplementary information (SI). Supplementary information is available. See DOI: **https://doi.org/10.1039/d5ma01002k**.

References

1 X. Li, Y. Zhou, S. Yu, G. Jia, H. Li and W. Li, *Energy*, 2019, **174**, 407–419.
2 S. Chen, G. Zhang, X. Xia, Y. Chen, S. Setunge and L. Shi, *Sustainable Energy Technol. Assess.*, 2021, **45**, 101212.
3 J. Wu, Z. Lian, Z. Zheng and H. Zhang, *Sustainable Cities Soc.*, 2020, **53**, 101893.
4 H. Duan, S. Chen and J. Song, *Energy*, 2022, **245**, 123290.
5 M. Bourdeau, X. Qiang Zhai, E. Nefzaoui, X. Guo and P. Chatellier, *Sustainable Cities Soc.*, 2019, **48**, 101533.
6 S. Seyedzadeh, F. P. Rahimian, I. Glesk and M. Roper, *Visualizat. Eng.*, 2018, **6**, 5.
7 I. G. Dino and C. M. Akgül, *Renewable Energy*, 2019, **141**, 828–846.
8 D. Ürge-Vorsatz, R. Khosla, R. Bernhardt, Y. C. Chan, D. Vérez, S. Hu and L. F. Cabeza, *Annu. Rev. Environ. Resour.*, 2020, **45**, 227–269.
9 X. C. Scanlon, United Nations Environment Programme Annual Report 2009, Nairobi, 2010.
10 J. Rosenow, P. Guertler, S. Sorrell and N. Eyre, *Energy Policy*, 2018, **121**, 542–552.
11 S. Kokoni and M. Leach, *Renewable Sustainable Energy Transition*, 2021, **1**, 100009.
12 A. Hu, S. Levis, G. A. Meehl, W. Han, W. M. Washington, K. W. Oleson, B. J. van Ruijven, M. He and W. G. Strand, *Nat. Clim. Change*, 2016, **6**, 290–294.
13 S. Roberts, *Energy Policy*, 2008, **36**, 4482–4486.
14 S. Schiavoni, F. D'Alessandro, F. Bianchi and F. Asdrubali, *Renewable Sustainable Energy Rev.*, 2016, **62**, 988–1011.
15 D. Densley Tingley, A. Hathway and B. Davison, *Build Environ.*, 2015, **85**, 182–189.

16 I. Siksnelyte-Butkiene, D. Streimikiene, T. Balezentis and V. Skulskis, *Sustainability*, 2021, **13**, 737.

17 T. Dickson and S. Pavía, *Renewable Sustainable Energy Rev.*, 2021, **140**, 110752.

18 W. Villasmil, L. J. Fischer and J. Worlitschek, *Renewable Sustainable Energy Rev.*, 2019, **103**, 71–84.

19 A. M. Borrero-López, V. Nicolas, Z. Marie, A. Celzard and V. Fierro, *Polymers*, 2022, **14**, 3974.

20 J. O. Akindoyo, M. D. H. Beg, S. Ghazali, M. R. Islam, N. Jeyaratnam and A. R. Yuvaraj, *RSC Adv.*, 2016, **6**, 114453–114482.

21 M. Joshi, B. Adak and B. S. Butola, *Prog. Mater. Sci.*, 2018, **97**, 230–282.

22 M. Szycher, *Szycher's Handbook of Polyurethanes*, CRC Press, 2012.

23 F. Hu, S. Wu and Y. Sun, *Adv. Mater.*, 2019, **31**, e1801001.

24 L. Glicksman, M. Schuetz and M. Sinofsky, *Int. J. Heat Mass Transfer*, 1987, **30**, 187–197.

25 P. J. Burns, L. C. Chow and C. L. Tien, *Int. J. Heat Mass Transfer*, 1977, **20**, 919–926.

26 M. S. Al-Homoud, *Build Environ.*, 2005, **40**, 353–366.

27 S. Alsoy, *J. Cell. Plast.*, 1999, **35**, 247–271.

28 H. Zhang, W.-Z. Fang, Y.-M. Li and W.-Q. Tao, *Appl. Therm. Eng.*, 2017, **115**, 528–538.

29 U. Berardi and M. Naldi, *Energy Build.*, 2017, **144**, 262–275.

30 M. T. Bomberg, M. K. Kumaran, M. R. Ascough and R. G. Sylvester, *J. Therm. Envelope Build. Sci.*, 1991, **14**, 241–267.

31 I. R. Shankland, *J. Cell. Plast.*, 1993, **29**, 114–131.

32 H. Fleurent and S. Thijs, *J. Cell. Plast.*, 1995, **31**, 580–599.

33 S. Wang, C. M. McGuirk, A. D'Aquino, J. A. Mason and C. A. Mirkin, *Adv. Mater.*, 2018, DOI: 10.1002/adma.201800202.

34 W. Lu, Z. Wei, Z. Y. Gu, T. F. Liu, J. Park, J. Park, J. Tian, M. Zhang, Q. Zhang, T. Gentle, M. Bosch and H. C. Zhou, *Chem. Soc. Rev.*, 2014, **43**, 5561–5593.

35 S. R. Batten, N. R. Champness, X.-M. Chen, J. Garcia-Martinez, S. Kitagawa, L. Öhrström, M. O'Keeffe, M. Paik Suh and J. Reedijk, *Pure Appl. Chem.*, 2013, **85**, 1715–1724.

36 N. Stock and S. Biswas, *Chem. Rev.*, 2012, **112**, 933–969.

37 A. Kirchon, L. Feng, H. F. Drake, E. A. Joseph and H. C. Zhou, *Chem. Soc. Rev.*, 2018, **47**, 8611–8638.

38 M. Ding, X. Cai and H. L. Jiang, *Chem. Sci.*, 2019, **10**, 10209–10230.

39 X. Liu, L. Zhang and J. Wang, *J. Materiomics*, 2021, **7**, 440–459.

40 Y. R. Lee, J. Kim and W. S. Ahn, *Korean J. Chem. Eng.*, 2013, **30**, 1667–1680.

41 F. Liang, D. Ma, L. Qin, Q. Yu, J. Chen, R. Liang, C. Zhong, H. Liao and Z. Peng, *Dalton Trans.*, 2024, **53**, 10070–10074.

42 Y. Zhang, H. Tan, J. Zhu, L. Duan, Y. Ding, F. Liang, Y. Li, X. Peng, R. Jiang, J. Yu, J. Fan, Y. Chen, R. Chen and D. Ma, *Molecules*, 2024, **29**(24), 5903.

43 P. Yan, Z. Chen, X. Li, F. Liang, Y. Tan, Y. Lin, K. Yang, C. Xiao, J. Wu and D. Ma, *J. Solid State Chem.*, 2024, **330**, 124461.

44 A. Pustovarenko, M. G. Goesten, S. Sachdeva, M. Shan, Z. Amghouz, Y. Belmabkhout, A. Dikhtiarenko, T. Rodenas, D. Keskin, I. K. Voets, B. M. Weckhuysen, M. Eddaoudi, L. C. P. M. de Smet, E. J. R. Sudhölter, F. Kapteijn, B. Seoane and J. Gascon, *Adv. Mater.*, 2018, **30**, 1–8.

45 D. J. Ashworth and J. A. Foster, *J. Mater. Chem. A*, 2018, **6**, 16292–16307.

46 Y. Zhang, X. Feng, S. Yuan, J. Zhou and B. Wang, *Inorg. Chem. Front.*, 2016, **3**, 896–909.

47 Z. Kang, L. Fan and D. Sun, *J. Mater. Chem. A*, 2017, **5**, 10073–10091.

48 E. Adatoz, A. K. Avci and S. Keskin, *Sep. Purif. Technol.*, 2015, **152**, 207–237.

49 W. Fan, X. Zhang, Z. Kang, X. Liu and D. Sun, *Coord. Chem. Rev.*, 2021, **443**, 213968.

50 H. Li, K. Wang, Y. Sun, C. T. Lollar, J. Li and H. C. Zhou, *Mater. Today*, 2018, **21**, 108–121.

51 R. E. Morris and P. S. Wheatley, *Angew. Chem., Int. Ed.*, 2008, **47**, 4966–4981.

52 H. Ren, J. Jin, J. Hu and H. Liu, *Ind. Eng. Chem. Res.*, 2012, **51**, 10156–10164.

53 S. Basu, A. Cano-Odena and I. F. J. Vankelecom, *J. Membr. Sci.*, 2010, **362**, 478–487.

54 A. Winkler-Skalna and B. Łoboda, *J. Build. Eng.*, 2020, **31**, 101348.

55 S. Peretz Damari, L. Cullari, R. Nadiv, Y. Nir, D. Laredo, J. Grunlan and O. Regev, *Composites, Part B*, 2018, **134**, 218–224.

56 H. Kim, Y. Miura and C. W. Macosko, *Chem. Mater.*, 2010, **22**, 3441–3450.

57 Y. Huo, C. Lin, H. Ge, P. Ying, M. Huang, P. Zhang, T. Yang, T. Wang, J. Wu, Y. Yan and V. Levchenko, *J. Polym. Res.*, 2023, **30**, 38.

58 J. Joy, J. Abraham, J. Sunny, J. Mathew and S. C. George, *Polym. Test.*, 2020, **87**, 106429.

59 S. Sharma, B. Pratap Singh, S. H. Hur, W. M. Choi and J. S. Chung, *Composites, Part A*, 2023, **166**, 107366.

60 C. Defonseka, Practical guide to flexible polyurethane foams practical guide to flexible polyurethane foams, 2013.

61 P. Bethevas, J. Bicerano, R. van den Bosch, J. Fosnaugh, R. de Genova, M. Brown, F. Casati, C. P. Christenson, P. Clavel and W. Farrissey, *Polymeric Foams: Mechanisms and Materials*, CRC Press LLC, 1st edn, 2004.

62 M. Ahmadi, S. Janakiram, Z. Dai, L. Ansaloni and L. Deng, *Membranes*, 2018, **8**, 50.

63 Z. Li, D. Zhan, A. Saeed, N. Zhao, J. Wang, W. Xu and J. Liu, *Dalton Trans.*, 2021, **50**, 8540–8548.

64 E. Stavitski, E. A. Pidko, S. Couck, T. Remy, E. J. M. Hensen, B. M. Weckhuysen, J. Denayer, J. Gascon and F. Kapteijn, *Langmuir*, 2011, **27**, 3970–3976.

65 M. Mihaylov, K. Chakarova, S. Andonova, N. Drenchev, E. Ivanova, A. Sabetghadam, B. Seoane, J. Gascon, F. Kapteijn and K. Hadjiivanov, *J. Phys. Chem. C*, 2016, **120**, 23584–23595.

66 A. Zárate, R. A. Peralta, P. A. Bayliss, R. Howie, M. Sánchez-Serratos, P. Carmona-Monroy, D. Solis-Ibarra, E. González-Zamora and I. A. Ibarra, *RSC Adv.*, 2016, **6**, 9978–9983.

67 M. Mubashir, Y. F. Yeong, K. K. Lau, T. L. Chew and J. Norwahyu, *Sep. Purif. Technol.*, 2018, **199**, 140–151.

68 M. Loloei, S. Kaliaguine and D. Rodrigue, *Sep. Purif. Technol.*, 2021, **270**, 118786.

69 T. K. Trung, P. Trens, N. Tanchoux, S. Bourrelly, P. L. Llewellyn, S. Loera-Serna, C. Serre, T. Loiseau, F. Fajula and G. Férey, *J. Am. Chem. Soc.*, 2008, **130**, 16926–16932.

70 C. G. Carson, K. Hardcastle, J. Schwartz, X. Liu, C. Hoffmann, R. A. Gerhardt and R. Tannenbaum, *Eur. J. Inorg. Chem.*, 2009, 2338–2343.

71 H. Zhao, B. Ding, E. Yang, X. Wang and X. Zhao, *Z. Anorg. Allg. Chem.*, 2007, **633**, 1735–1738.

72 T. Loiseau, C. Serre, C. Huguenard, G. Fink, F. Taulelle, M. Henry, T. Bataille and G. Férey, *Chem. – Eur. J.*, 2004, **10**, 1373–1382.